

## PREDICTING SURFACE FOREST FUELS ON THE CERRADO IN CANTÃO STATE PARK FROM AIRBORNE RGB SENSOR IMAGES

Igor Viana Souza<sup>1</sup>, Hygor Gomes de Almeida Sousa<sup>2</sup>, Aline Silvestre Pereira Dornelas<sup>3</sup>, Antonio Carlos Batista<sup>4</sup>, Gil Rodrigues dos Santos<sup>5</sup>, Marcos Giongo<sup>6</sup>

<sup>1</sup> Centro de Monitoramento Ambiental (CeMAF), Universidade Federal do Tocantins - UFT, Gurupi, Tocantins, Brasil - igor.souzavigor@gmail.com

<sup>2</sup> Centro de Monitoramento Ambiental (CeMAF), Universidade Federal do Tocantins - UFT, Gurupi, Tocantins, Brasil - hygoralmeida.floresta@outlook.com

<sup>3</sup> Centro de Monitoramento Ambiental (CeMAF), Universidade Federal do Tocantins - UFT, Gurupi, Tocantins, Brasil - eng.alinesilvestre@gmail.com

<sup>4</sup> Universidade Federal do Paraná, Programa de Pós-Graduação em Engenharia Florestal, Curitiba, Paraná, Brasil - batistaufpr@gmail.com

<sup>5</sup> Universidade Federal do Tocantins, Programa de Pós-Graduação em Produção Vegetal, Gurupi, Tocantins, Brasil - gilrsan@mail.uft.edu.br

<sup>6</sup> Centro de Monitoramento Ambiental (CeMAF), Universidade Federal do Tocantins - UFT, Gurupi, Tocantins, Brasil - giongo@uft.edu.br

Received for publication: 29/11/2022 – Accepted for publication: 11/05/2023

### Resumo

*Predição do material combustível superficial de cerrado no parque estadual do cantão a partir de imagens de sensor RGB aerotransportado.* A quantificação do material combustível em área típica do Cerrado é limitada pela dificuldade em obtenção de dados, pelos altos custos e pelo elevado gasto em campo. Em busca de alternativas que facilitem a obtenção dos dados, a estimativa indireta vem sendo aplicadas, resultando equações locais para a predição da carga em função de variáveis de fácil obtenção. Nesse contexto, buscou-se desenvolver equações locais para estimar a carga de material combustível, em área de Cerrado, no Parque Estadual do Cantão - Tocantins, em função de variáveis mensuradas em campo e variáveis digitais provenientes do processamento de imagens digitais RGB (Red, Green and Blue) adquiridas por meio de aerolevantamentos. Com o processamento das imagens digitais, extraiu-se as seguintes variáveis: altura média no modelo digital (hMDA) e densidade de pontos no modelo tridimensional (DPM). Após o levantamento aéreo, realizou-se a amostragem em campo, coletando as seguintes variáveis: altura média em campo (hc), quantidade de indivíduos (Qt) e Material Combustível Total (MCT). Posteriormente, foram ajustadas equações, adotando todo o conjunto amostral. O critério de seleção do modelo foi com base ao  $R^2_{aj}$ , Syx% e gráfico de resíduos, em que foram obtidos coeficiente de determinação ajustados ( $R^2_{aj}$ ) de 0,12 a 0,83 e Erro padrão residual (Syx%) de 19,4 a 44%. Foram observados que o uso de pontos de controle realizado pelo MDA reduz a ocorrência de erros, as correlações entre as variáveis analisadas indicam a importância de considerar múltiplos fatores ao realizar análises e predições nas áreas de estudo.

**Palavras-chave:** Sensoriamento Remoto, incêndios florestais, modelagem

### Abstract

*Predicting surface forest fuels on the cerrado in Cantão state park from airborne RGB sensor images.* Forest fuel quantification in a typical Cerrado area is difficult due to the high costs and long field times associated with collecting data. In search of alternatives that facilitate data collection, indirect estimation has been studied, resulting in local equations for predicting the load based on easily obtainable variables. In this context, we sought to develop local equations to estimate the load of forest fuel, in a Cerrado area, in the Cantão Park State – Tocantins. As a function of variables measured in the field and digital variables from the processing of RGB digital images (Red, Green and Blue) acquired through aerial surveys. With the processing of digital images, the following variables were extracted: mean height in the digital model (hMDA) and point density in the three-dimensional model (DPM). After the aerial survey, field sampling was carried out, collecting the following variables: mean height in the field (hc), number of individuals (Qt) and Total Fuel Material (MCT). Subsequently, equations were fitted, adopting the entire sample set. The model selection criterion was based on  $R^2_{aj}$ , Syx% and residual graph, in which adjusted coefficient of determination ( $R^2_{aj}$ ) from 0.12 to 0.83 and residual standard error (Syx%) of 19.4 were obtained at 44%. It was observed that the use of control points performed by the MDA reduces the occurrence of errors, the correlations between the analyzed variables indicate the importance of considering multiple factors when performing analyzes and predictions in the study areas.

**Keywords:** Remote Sensing, forest fires, modelling.

## INTRODUCTION

A prominent characteristic of the Cerrado biome is the accumulation of herbaceous and woody fuels. Soares *et al.* (2017) consider forest fuel to be all living or dead organic material capable of combustion (e.g. twigs, branches, fallen trunks, grasses, herbs, shrubs, humus, and peat) that are produced naturally or under anthropogenic

pressures (e.g. logging) above or below the forest floor, and can be assessed according to quantity, type, and arrangement.

The amount of forest fuel in the Cerrado varies from grams to tonnes per hectare and is expressed by the term "load", which refers to the amount of oven-dry matter per unit area, it influenced mainly by the type, spacing, age of the vegetation and anthropogenic activities (SOARES *et al.*, 2017). The load of the forest fuel is directly correlated with the intensity of the fire. According to Soares *et al.* (2017), around 1,2 t.ha<sup>-1</sup> of fine, dry forest fuel becomes sufficient for the spread of fire and, with the accumulation of forest fuel in conditions favourable to fire, can result in the spread of forest fires to disastrous levels.

Determining forest fuel load is a significant factor in forest fire prevention planning and relevant in modelling fire behaviour (SANTOS *et al.*, 2019). In order to obtain quantitative information on forest fuel, the destructive method can be employed, which involves sampling forest fuels at predetermined intervals or randomly distributed intervals using templates of different sizes and shapes (e.g. rectangular and quadrangular) (GRIEBELER *et al.*, 2020; TAVARES, 2017; SANTOS *et al.*, 2019; SOUZA *et al.*, 2018; WHITE *et al.*, 2013).

However, the destructive sampling method is considered complex due to the spatiality of the forest fuel on site. In addition, in large areas the survey becomes technically and financially unfeasible (DUFF *et al.*, 2012). As a result, other methods have been studied and implemented, such as indirect estimates, in which local equations are developed to estimate the load as a function of easily obtained variables (e.g. height, blanket thickness, diameter and number of individuals) (SANTOS *et al.*, 2019; SOUZA *et al.*, 2018; BENDIG *et al.*, 2014; JANNOURA *et al.*, 2015).

Among indirect methods, digital image processing is also notable, which is widely applied in precision agriculture. Particularly, UAVs (Unmanned Aerial Vehicles) are used as platforms that are capable of integrating high-resolution sensors to obtain digital images, thereby enabling the extraction of various vegetation parameters (such as height, biomass, and vegetation index) (CUNLIFFE *et al.*, 2020; PANDAY *et al.*, 2020; HARKEL *et al.*, 2019), as well as data that can be used to determine the load of forest fuel using statistical models (SANTOS *et al.*, 2019).

In this context, statistical models are essential tools, since quantifying the load of forest fuel is fundamental to carrying out any fire management procedure. Thus, using biophysical variables to fit regression equations can reduce difficult processes in the field, such as time spent travelling in areas that are difficult to access (SOUZA *et al.*, 2018).

Determining the forest fuel load using equations is still scarce. The main studies in Brazil have been carried out on pine, eucalyptus and araucaria plantations, located in the Atlantic Forest biome in the southern region (e.g. BEUTLING *et al.*, 2012; BEUTLING *et al.*, 2006; RIBEIRO; SOARES, 1998). However, there is a lack of studies on the Cerrado biome, where some of the studies that have addressed the modelling of forest fuel in the Cerrado biome were carried out by Santos *et al.* (2019), Santos *et al.* (2021) and Souza *et al.* (2018).

In that sense, this research assumes that: i - flight parameters interfere with the quality of the products generated after data processing; ii - the use of Ground Control Point - GCP in georeferencing the images interferes with the quality of the products generated after data processing; 3 - there is a relationship between the predictor variables studied and the total forest fuel load (MCT).

The purpose of this paper was to develop local equations to estimate forest fuel load of as a function of variables measured in the field and digital variables from the processing of RGB digital images acquired through aerial surveys in the Cantão State Park in the state of Tocantins.

## MATERIAL AND METHODS

### Experiment location: Cantão State Park (PEC)

The research was carried out at four sites in the northern region of the Cantão State Park (PEC) in the state of Tocantins. The PEC is an integral protection conservation unit, part of the State Conservation Unit System (SEUC), covering an area of approximately 90,000 hectares, located at the geographical coordinates S10°26'33" latitude, W49°10'56" longitude, involving the municipalities of Pium and Caseara, in Tocantins (Figure 1).

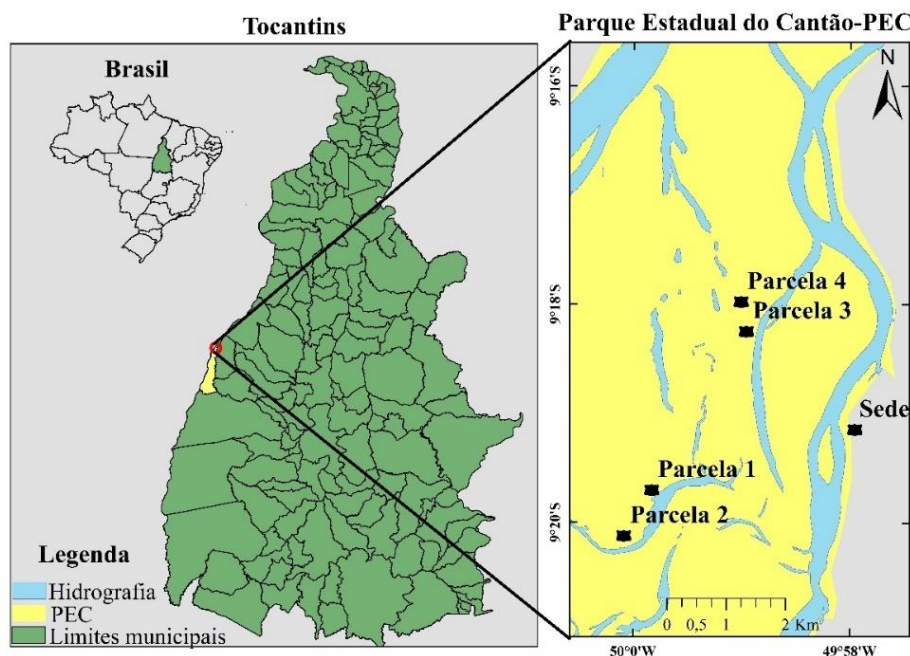


Figure 1. Location of study areas in Parque Estadual do Cantão, Tocantins.

Figura 1. Localização das áreas de estudo no Parque Estadual do Cantão, Tocantins.

According to the Köppen climate classification, the region's predominant climate is type C2wA'a' - a humid sub-humid climate with moderate water deficiency in winter, annual potential evapotranspiration mean is 1,500 mm, distributed in the summer at around 420 mm over the three consecutive months with the highest temperature, the summer is rainy and occurs between the months of October and April, and the dry winter takes place from May to September (SEPLAN 2012; NATURATINS, 2019).

The study location is characterised as a recovery area, made up of areas of alluvial semideciduous seasonal forest, considerably anthropised in a Cerrado area (SEPLAN, 2016), with the presence of the predominant herbaceous species Capim-sapê (*Imperata brasiliensis* Trin.) and Canarana (*Hymenachne amplexicaulis* (Rudge) Nees), both belonging to the Poaceae family.

#### Planning, sub-plots distribution and Ground Control Points (GCP) selection

The aerophotogrammetric planning survey was subdivided into 3 stages: (1) distribution of the sub-plots and selection of the GCP and collection of the coordinates with a geodetic receiver; (2) execution of the flight plan and collection of the forest fuel; (3) three-dimensional reconstruction of the areas and preparation of the digital models.

The plots were established using geoprocessing and remote sensing techniques, with a view to the logistics of travelling to the plots and critical fire areas, identified by analysing the hydrography and the scars of burning in the PEC. As a result, 77 sub-plots were installed throughout the experiment, with 22 sub-plots being distributed in plots 1, 2 and 3, while 11 plots were distributed in plot 4.

Each plot had a rectangular area of 4.5 hectares ( $150 \times 300$  m), where sub-plots measuring  $0.25 \text{ m}^2$  ( $0.5 \times 0.5$  m) were systematically distributed. The size of the sub-plot was chosen with a view to wide sampling and increasing the variability of the fuel sampled.

To demarcate the sub-plots, artificial targets made from  $0.5 \times 0.5$  metre boards were distributed, making them identifiable in the images. In addition, 12 sub-plots were selected as GCP.

#### Flight plan execution and forest fuel collection

The flight was carried out using a DJI Phantom 4 multirotor with an RGB sensor measuring 1/2.3" with a resolution of  $4,000 \times 3,000$  pixels and a focal length of 4.73 mm. The flight heights were 75 and 100 metres, considered as treatments, and 85% longitudinal and 85% lateral coverage was adopted for the experiment. The flight plan resulted in a spatial resolution of 2.5 cm and 3.4 cm (Ground Sample Distance - GSD), for flight heights of 75 and 100 metres respectively.

After the flights, the mean height of the vegetation from the centre of the sub-plot in centimetres (hc) was collected in each sub-plot. The surface forest fuel was then collected using the destructive method, separating the material into the following classes: live herbaceous, dead herbaceous and total herbaceous fuels.

The number of individuals present (Qt) was also quantified using the bases of the stalks identified close to the ground after the forest fuel had been collected.

Each fraction of surface forest fuel was weighed in the field to obtain a wet mass. Subsequently, they were separated into sub-samples of approximately 100g, packed and identified in kraft paper bags and dried in an oven at 70°C until they reached a constant mass. Finally, the moisture content of the superficial forest fuel was calculated using the equation:

$$U = \frac{(MU-MS)}{MS} * 100$$

Where: U, moisture content of forest fuel (%); MU, wet mass of the material at the time of collection (g); MS, dry mass of the material after heating (g).

With the moisture content of the sub-sample, it was possible to determine the load of forest fuel for each sub-plot, in t.ha<sup>-1</sup>. In this way, the sum of the fractions of the forest fuel load can be referred to in this study as the Total Forest fuel (TCM) load.

### Three-dimensional reconstruction and digital model preparation

After executing the flight plan, the images were pre-aligned using the Structure From Motion (SfM) algorithm, and then the GCP coordinates were entered using Agisoft Metashape software. At this stage, 2 treatments were considered in the three-dimensional reconstruction: treatment 1 - without the use of 0 GCP; treatment and treatment 2 - 6 GCP.

The coordinates of the GCP were inserted into the same software using the coordinates as a reference, transporting these known coordinates to the images and georeferencing the block of images.

The three-dimensional models of each plot were imported into the SAGA GIS software version 7.8.1 to create the Digital Surface Model (DSM), Digital Terrain Model (DTM) and Digital Height Model (resulting from the subtraction between DSM and DTM). The three-dimensional model was also used to generate a new variable called density of points in the model (DPM), which refers to the number of points in an area extrapolated to hectares.

Subsequently, the average height data in the digital height model (hMDA), obtained from the difference between MDS and MDT, and the density of points in the model (DPM), were extracted and tabulated using GIS software for each sub-plot.

### Statistical analysis

An exploratory analysis of the MCT field data was carried out in order to identify and remove possible outliers in the sampling.

The data was descriptively analysed using the mean vegetation height (hc), the number of MCT individuals (Qt) and the frequency of these individuals. Due to the different sample sizes of the groups, the means were compared using the Tukey-Kramer test to identify significant differences ( $p < 0.05$ ). The same procedure for analysing variance and comparing means was used for the entire sample set.

Pearson's correlation analyses were carried out between the hc and Qt variables and the hMDA and DPM digital variables, which were considered significant at  $p < 0.05$ ;  $p < 0.01$ . Correlations were then made between the dependent variable MCT and the field variables hc and Qt for each plot, and for the digital variables of the treatment with the best correlations of hMDA and DPM, and with its respective control.

After analysing the correlation, the variables that showed significant correlations with  $p < 0.05$ ;  $p < 0.01$  were selected for the adjustment of regression equations for each plot, using the Stepwise adjustment method, taking into account the dependent variable MCT in t.ha<sup>-1</sup> and the independent variables hc and Qt and the digital variables hMDA and DPM, with their respective transformations  $x^2$ ,  $x^3$ , Log (x), Root (x), Ln (x), 1/x and X1\*X2. As an additional analysis, the correlation and regression were subjected to their respective analyses again, using the entire sample set. The equations were selected based on the values of the coefficient of determination (R<sup>2</sup>aj) and standard error of the estimate in percentage (Syx%) and the graphical analysis of the residuals (goodness-of-fit indices). Finally, the residues was subjected to the normality and homogeneity test (Shapiro-Wilk) considering  $p < 0.05$ . All the steps described were carried out using the R software (version 4.1.0).

## RESULTS

According to Table 1, there was considerable variation in the characteristic means ( $\bar{y}$ ). This variation is indicated by the difference between the means and suggests that the samples have different levels of each characteristic. In addition, the description of the variation in the coefficients of variation (CV%) across the plots

for each trait indicates that there is great variability between the samples for each characteristic. This variability can be explained by various factors, such as soil and species variation.

Table 1. Statistical summary of sample characteristics.

Tabela 1. Resumo estatístico das características da amostra.

Plot	n	Specie	FrA	Fr%		MCT (t.ha <sup>-1</sup> )	hc (cm)	Qtí (ind.ha <sup>-1</sup> )
1	17	<i>I. brasiliensis</i>	17	100	ȳ	21.8	14.4	1,070,588
					CV%	50.1	40.5	27.7
2	21	<i>I. brasiliensis</i>	21	100	ȳ	21.8	17.6	892,000
					CV%	62.32	44.9	45.9
3	20	<i>I. brasiliensis</i>	15	75	ȳ	19.3	17.3	2,180,952
					CV%	48.2	29.8	58
4	11	<i>H. amplexicaulis</i>	11	100	ȳ	33.4	19.1	1,043,636
					CV%	37.6	23.7	57.2
<b>Total</b>	<b>69</b>	<i>I. brasiliensis</i>	<b>53</b>	<b>76.8</b>	ȳ	<b>22.7</b>	<b>16.9</b>	<b>5,186,816</b>
		<i>H. amplexicaulis</i>	<b>16</b>	<b>23.2</b>	CV%	<b>51</b>	<b>36.3</b>	<b>58.1</b>

Where: FrA, absolute frequency; Fr%, relative frequency; ȳ mean; CV% coefficient of variation; n, number of samples; TCM, Total Forest fuel; hc, average height in the field; Qtí, number of individuals.

When evaluating the results in Table 2, it can be seen that for hMDA, for the 75 m flight in plot 1, the treatments were statistically equal, while the other plots were statistically different compared to the control. In GPC treatment 6, it was observed that flight altitude had no significant impact on hMDA values (Table 2). Therefore, to optimise efficiency and save time, it is recommended to fly at an altitude of 100 metres, except for plot 4. However, it is important to emphasise that this recommendation does not apply to plot 4, where it may be necessary to fly at a different altitude to obtain the desired results.

Table 2. Means comparison by using the Tukey-Kramer test for the hMDA variable.

Tabela 2. Comparação de médias pelo teste Tukey-Kramer para variável hMDA.

Variable	Plot	Flight / voo (m)	0 GCP	6 GCP	Control (hc)	
hMDA	1	75	13.5 Ba	13.3 Aa	14.4 a	
		100	9.3 Aa	12.8 Ab	14.4 c	
	2	75	8.7 Aa	9 Aa	17.6 b	
		100	11.2 Ba	10Aa	17.6 b	
	3	75	8.1 Ab	6.7 Aa	17.33 c	
		100	8 Aa	7.3 Aa	17.33 b	
	4	75	13.5 Ab	11 Ba	22.36 c	
		100	17.5 Bb	9.8 Aa	22.36 c	
<b>TOTAL</b>		<b>75</b>	<b>9.8 Aa</b>	<b>9.7 Aa</b>	<b>16.9 b</b>	
		<b>100</b>	<b>10.7 Aa</b>	<b>10.1 Aa</b>	<b>16.9 b</b>	

Where: GCP = Ground Control Point; hMDA = mean height in the digital model.

After examining the data relating to the DPM variable in different 75 and 100 metre flights (Table 3), in which the 0 GPC treatment was used, it was found that only the first portion of the 75 metre flight and the fourth portion of the 100 metre flight showed statistically similar results to their respective control groups. This means that the other flight plots showed statistically significant differences compared to the controls, indicating that the application of the treatment had a different effect to what was expected.

Table 3. Means comparison of using the Tukey-Kramer test for the DPM variable.

Tabela 3. Comparação de médias pelo teste Tukey-Kramer para variável DPM.

Variable	Plot	Flight/voo (m)	0 GCP	6 GCP	Control (hc)	
DPM	1	75	1.3E+06 Bb	7.5E+05 Aa	1.0E+06 b	
		100	7.2E+05 Aa	7.2E+05 Aa	1.0E+06 b	
	2	75	1.2E+06 Ba	1.1E+06 Ba	8.9E+05 b	
		100	6.3E+05 Aa	6.3E+05 Aa	8.9E+05 b	
	3	75	1.0E+06 Ba	1.1E+06 Ba	2.1E+06 b	
		100	6.0E+05 Aa	6.2E+05 Aa	2.1E+06 b	
	4	75	6.4E+05 Aa	7.7E+05 Aa	1.0E+06 b	
		100	8.1E+05 Bb	7.6E+05 Aa	1.0E+06 b	
<b>TOTAL</b>		<b>75</b>	<b>6.7E+05 Aa</b>	<b>9.8E+05 Ab</b>	<b>1.3E+06 c</b>	
<b>TOTAL</b>		<b>100</b>	<b>6.7E+05 Aa</b>	<b>1.1E+06 Ab</b>	<b>1.3E+06 c</b>	

 Where: GCP = *Ground Control Point*; DPM = point density in the three-dimensional model.

Table 4 shows the coefficient of determination ( $r^2$ ) for the respective treatments. It was observed that the GCP 6 treatment showed statistically significant results, with  $r^2$  variations between 0.57 and 0.85, with plot 1 standing out with an  $r^2$  of 0.85.

On the other hand, the GCP 0 treatment showed a weak correlation with hc, except in plot 4, which showed an  $r^2$  of 0.55, significant at a 5% probability level. Furthermore, when considering the entire sample set ( $n = 69$ ), there was a reduction in the relationship between hc and hMDA, resulting in an  $r^2$  of 0.57, which is still considered significant at a 1% probability level. Concerning the Qti variable, there was no significant correlation with DPM, according to the analysis of residuals and the comparison of means.

Table 4. Pearson's correlation analysis for variable hc and Qti.

Tabela 4. Análise de correlação de Pearson para variável hc e Qti.

Plot	Variable	hMDA (0 GCP)	hMDA (6 GCP)	Plot	Variable	DPM (0 GCP)	DPM (6 GCP)
hc	1	0.15	0.85***	1		0.09	0.32
	2	0.23	0.67**	2	Qtí	0.2	0.29
	3	0.25	0.63**	3		0.3	0.1
	4	0.55*	0.65**	4		0.3	0.32
<b>Total</b>		<b>0.3</b>	<b>0.57**</b>	<b>Total</b>		<b>0.3</b>	<b>0.12</b>

Where: GCP = *Ground Control Point*; hMDA = mean height in the digital model; DPM = point density in the three-dimensional model. \* significant at 5% probability; \*\* significant at 1% and \*\*\* significant at 0.1% probability.

Table 5 shows the degree of Pearson's correlation between the MCT variable and the hc and hMDA variables for the GPC 6 treatment on the 100 m flight. When evaluating the relationship between fuel material and hc, a strong relationship was observed between height and fuel material load, ranging from  $r = 0.60$  to  $r = 0.85$ . hMDA also showed better correlations with fuel load, ranging from 0.60 to 0.90, except for plot 4, where there was no significant relationship. When considering the entire sample set in the analysis ( $n = 69$ ) there was a reduction in the relationship, however, it was considered significant at the 0.1% probability level.

Table 5. Correlation analysis for MCT variable.

Tabela 5. Análise de correlação de Pearson para variável MCT.

Plot	Variable	hc	hMDA (6 GCP)
1	MCT	0.85***	0.90***
2		0.62**	0.75***
3		0.64**	0.65**
4		0.80**	0.19
<b>Total</b>		<b>0.60**</b>	<b>0.60**</b>

Where: hMDA = mean height in the digital model; hc = mean height in the field; MCT = Total Forest fuel. \* significant at 5% probability; \*\* significant at 1% and \*\*\* significant at 0.1% probability.

Given the importance of the relationship between MCT and the field and digital variables, regression analyses were carried out to predict the forest fuel. The goodness-of-fit and accuracy statistics of the models selected using the *Stepwise* method are shown in Table 6.

The equations generated with the hMDA predictor showed great relevance for plots 1 and 2, with values of  $p < 0.001$  and  $R^2aj = 0.82$  and  $R^2aj = 0.62$ , respectively. Although the hMDA predictor in the equation generated for plot 3 was significant with a value of  $p < 0.05$ , it showed fitting results with  $R^2aj = 0.33$  and a high residual with  $Syx\% = 39.2$ . Plot 4 fitted the DPM variable in its equation; however, the addition of the predictor was not significant and showed the lowest goodness-of-fit values among plots, with  $R^2aj = 0.09$  and  $Syx\% = 40.5$ .

When evaluating the hc predictor, in all situations the regression equations obtained values of  $p < 0.001$ , i.e. the addition of the predictors was significant and related to changes in the response variable. For the fitted equations, the coefficient of determination ranged from  $R^2aj = 0.39$  to  $R^2aj = 0.70$  and the  $Syx\%$  ranged from 20 to 34.2, with plots 1 and 4 having higher  $R^2aj$  and  $Syx\%$  statistics than the other plots.

When the equation was fitted for the entire sample set ( $n=69$ ), the hc variable stood out when compared to hMDA with  $R^2aj = 0.7$  and  $R^2aj = 0.48$ , respectively. Also, looking at the relationship between observed and estimated values in Figure 2, it can be seen that using the hc predictor, the values are closer to the trend line when compared to the hMDA predictor.

Table 6. Regression analysis and goodness-of-fit for MTC prediction.

Tabela 6. Análise de regressão e estatísticas de qualidade das equações para predição de MTC.

Plot	Y	X	Coefficient	R <sup>2</sup>	R <sup>2</sup> aj	Syx%	F (interaction)
1	MCT	β0	2.296	0.83	0.82	21.6	77.3(p<0,001)
		hMDA	1.46***				
2	MCT	β0	13.12***	0.62	0.6	30	29.6(p<0,001)
		hMDA <sup>2</sup>	0.065***				
3	MCT	β0	3.75	0.33	0.32	39.2	10.2(p<0,05)
		hMDA	2.13*				
4	MCT	β0	45	0.09	0	40.5	0.42(p<0,668)
		1/DPM	4498621				
		Raiz (DPM)	-0.007				
Plot	Y	X	Coefficient	R <sup>2</sup>	R <sup>2</sup> aj	Syx%	F (interaction)
1	MCT	β0	-20.148	0.78	0.7	24.29	40.4(p<0,001)
		hc	1.5978***				
2	MCT	β0	13.631	0.55	0.48	31.22	18.6(p<0,001)
		hc <sup>3</sup>	0.001*				
3	MCT	β0	9.401*	0.42	0.39	34.2	13.7(p<0,001)
		hc <sup>2</sup>	0.031***				
4	MCT	β0	-51.93	0.75	0.69	20	20.6(p<0,001)
		RAIZ (hc)	18.17***				
Total	MCT	β0	6.16**	0.49	0.48	35	64.3(p<0,001)
		hMDA	1.54***				
	MCT	β0	-2.24	0.75	0.7	25	166.2(p<0,001)
		hc	1.42***				

Where: R<sup>2</sup>aj = adjusted coefficient of determination; Syx% = standard error in percentage; hMDA = mean height in the digital model; hc = mean height in the field; MCT = Total Forest fuel; R<sup>2</sup> = coefficient of determination; DPM = density of points in the three-dimensional model. \* significant at 5% probability; \*\* significant at 1% and \*\*\* significant at 0.1% probability.

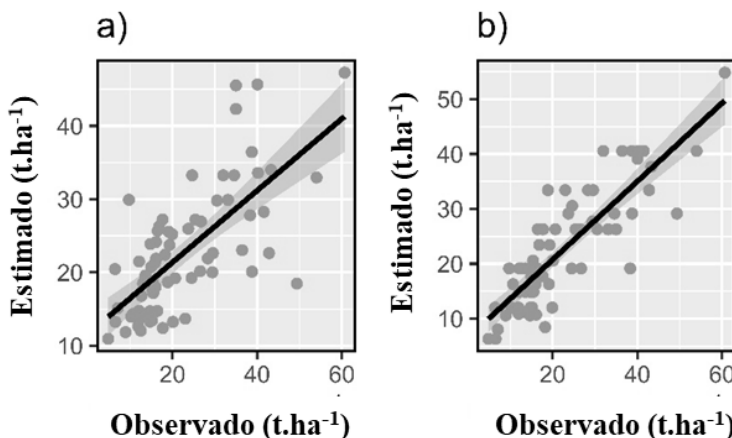


Figure 2. Observed versus predicted linear regression for the entire sample set. a) refers to the use of the hMDA variable to predict the load of forest fuel; b) refers to the use of the variable hc to predict the load of forest fuel (t.ha<sup>-1</sup>); confidence interval represented in shaded on the trend line.

Figura 2. Regressão linear observado versus estimado para todo conjunto amostral. a) refere-se ao uso da variável hMDA para estimar a carga de material combustível; b) refere-se ao uso da variável hc para estimar a carga de material combustível (t.ha<sup>-1</sup>); intervalo de confiança representado em sombreado na linha de tendência.

## DISCUSSION

Table 1 shows a high degree of dispersion of data in relation to the mean. According to Rossi (2020), reducing data variability reduces standard deviation and improves analysis accuracy. Although sampling variability is difficult to reduce when vegetation is heterogeneous, as it is in the Cerrado. In order to ensure that the values of the interest variable vary slightly from one sample to another, Pelliccino Netto and Brenna (1997) recommend dividing heterogeneous populations into homogeneous strata.

When evaluating the results in Table 2, several factors affect the accuracy of the products, among which the number of GCP and their distribution in the study area are especially significant (MARTÍNEZ-CARRICONDO *et al.*, 2018). These same authors noted in their research that among the distributions evaluated, the most reliable results were obtained with the combination of GCP distribution at the edges and distribution stratified by the interior of the study region.

It can also be seen that the hMDA averages are lower than the hc values, characterising an underestimation of height. The same pattern was observed by Bendig *et al.* (2014), using images based on airborne RGB sensors to estimate the height of cultivars in agriculture.

Although the analyses of the means presented in Table 2 shows that in most cases hMDA was statistically different to hc, the variable hc and hMDA showed strongly significant correlations in all situations (Table 4). The relationship between actual and predicted height was observed by the authors Bendig *et al.* (2014) and Han *et al.* (2018), in which strong linear correlations were found with coefficients of determination ranging from 0.72 to 0.92.

Looking at the correlation values (Table 5), we note the importance of the height and MCT relationship. The most predominant species sampled in the experiment (*H. amplexicaulis* and *I. brasiliensis*) are C4 metabolism plants that grow upright and straight, respectively. C4 grasses are plants with a high photosynthetic rate, favoured mainly in high light and temperature environments, and this characteristic allows for a greater increase in biomass per unit of time (TAIZ; ZEIGER, 2017). In addition, Bendig *et al.* (2014) and SOUZA *et al.* (2018) showed significant relationships between height and dry mass, making the premise suitable for estimating the load of forest fuel employing height.

The equations fitted to predict forest fuel in the different plots performed similarly to Pearson's correlations when using the hc, hMDA and DPM predictors, with the highest coefficient of determination being found in plot 1, in the fit in which the hMDA variable was selected. Plot 4, on the other hand, had the worst results in terms of both correlation and regression when the variable DPM was selected, and the same low results were found in plot 3.

During the sampling of plots 1 and 3, the species *Hymenachne amplexicaulis* was found, which is characterised by its high rate of dry mass accumulation in short time intervals, as previously reported, and, when observing the graph of observed versus estimated values in Figure 2, it can be seen that the greatest distance of the

values from the mean trend line is located mainly in regions of greater accumulation of forest fuel, in accordance with the idea that both the height and the number of individuals are not sufficient to explain the MCT of the species *H. amplexicaulis*.

Santos *et al.* (2021) worked with relationships and modelling of the surface forest fuel of the grassland savannah in the Jalapão region - Tocantins, and fitted linear regression equations with herbaceous height, blanket height, number of individuals and number of species. They found that the best equations for prediction of dead herbaceous material and herbaceous material were fitted with herbaceous height and blanket height,  $R^2_{aj} = 0.63$ ;  $Syx\% = 39.05$  and  $R^2_{aj} = 0.73$ ;  $Syx\% = 28.92$ , respectively.

The vegetation heterogeneity and the difficulty of access to certain areas can affect the quality and representativeness of the samples collected. This in turn can affect the statistical analyses carried out. To overcome these limitations, it is important to adapt the sampling strategy to the environment concerned. For instance, it is possible to divide the area into smaller, more homogeneous units and randomly sample within each of these units. Another workaround is to use specific sampling methods for each vegetation type or terrain, such as transects or fixed plots.

Our results show that it is possible to use unmanned aerial vehicles (UAVs) to estimate total forest fuel load. It is therefore a tool that has proved effective in situations where there is a need for faster field analysis. As long as it is affordable and can be done in different types of phytogeographies, it can be used at any time of the year. Further studies are suggested to evaluate the effectiveness of using UAVs by assessing the representativeness of the sample in relation to the total population and taking into account other sources of variation, such as climatic conditions and seasonality, to ensure the reliability of the results obtained.

## CONCLUSION

- The input variables hc and Qti, digital variables hMDA and DPM showed positive correlations for building regression models to predict the total forest fuel load.
- Control points used by the MDA during georeferencing ensure more accurate results and reduce the errors possibility.
- Additionally, flight height does not influence hMDA values, which is helpful when choosing the ideal height for surveying.
- Lastly, correlations between variables indicate the importance of considering multiple factors in the analysis and prediction of the study areas.

## REFERENCES

BENDIG, J.; YU, K.; AASEN, H.; BOLTEN, A.; BENNERTZ, S.; BROSCHET, J.; GNYP, L. M.; BARETH, G. Combining UAV-based plant height from crop surface models, visible and near infrared vegetation indices for biomass monitoring in barley. **International Journal of Applied Earth Observation and Geoinformation**, Amsterdam, v. 39, p. 79 - 87, 2014.

BEUTLING, A.; BATISTA, A. C.; SOARES, R. V.; VITORINO, M. D. Characterization and modeling of forest fuels in Araucaria angustifolia plantations. **Forest Ecology and Management**, Amsterdam, v. 234, p. 1-9, 2006.

BEUTLING, A.; BATISTA, A. C.; STOLLE, L.; TETTO, A. F.; ALVES, M. V. G. Caracterização e modelagem de material combustível superficial em povoamentos de *Pinus elliottii*. **Floresta**, Curitiba, v. 42, n. 3, p. 443 - 452, 2012.

CUNLIFFE, A. M.; ASSMANN, J. J.; DASKALOVA, G. N.; KERBY, J. T.; MYERS-SMITH, I. H. Aboveground biomass corresponds strongly with drone-derived canopy height but weakly with greenness (NDVI) in a shrub tundra landscape. **Environmental Research Letters**, Bistol, v. 15, n. 12, p. 1 - 16, 2020.

DUFF, T. J.; BELL, T. L.; YORK, A. Predicting continuous variation in forest fuel load using biophysical models: a case study in south-eastern Australia. **International Journal of Wildland Fire**, Melbourne, v. 22, p. 318 - 332, 2012.

GRIEBELER, A. M.; TURCHETTO, F.; RORATO, D. G.; SCHUMACHER, M. V.; FACCO, A. T.; PORAZZI, A. V. Caracterização quali-quantitativa do material combustível e estoque de carbono em vegetação de capoeira, Santa Maria, **Brazilian Journal of Development**, São José dos Pinhais, v. 6, n. 3, p. 11038 - 11046, 2020.

HAN, W. S.; GRAHAM, J. P.; CHOUNG, S.; PARK, E.; CHOI, W.; KIM, Y. S. Local-scale variability in groundwater resources: Cedar Creek Watershed, Wisconsin, U.S.A. **Journal of Hydro-environment Research**, Amsterdam, v. 20, p. 38 - 51, 2018.

HARKEL, J. T.; BARTHOLOMEUS, H.; KOOISTRA, L. Biomass and crop height estimation of different crops using UAV-based Lidar. **Remote Sensing**, Basel, v. 12, n. 1, p. 1 - 18, 2020.

JANNOURA, R.; BRINKMANN, K.; UTEAU, D.; BRUNS, C.; JOERGENSEN, R. G. Monitoring of crop biomass using true colour aerial photographs taken from a remote controlled hexacopter. **Biosystems Engineering**, Amsterdam, v. 129, p. 341 - 351, 2015.

MARTÍNEZ-CARRICONDO, P.; AGÜERA-VEGA, F.; CARVAJAL-RAMÍREZ, F.; MESAS-CARRASCOSA, F. J.; GARCÍA-FERRER, A.; PÉREZ-PORRAS, F. J. Assessment of UAV-photogrammetric mapping accuracy based on variation of ground control points. **International journal of applied earth observation and geoinformation**, Amsterdam, v. 72, p. 1 - 10, 2018.

NATURATINS – Instituto Natureza do Tocantins. **Parque Estadual do Cantão completa seu 21º ano de criação**. 2019. Disponível em: <https://www.to.gov.br/naturatins/noticias/parque-estadual-do-cantao-completa-seu-21o-ano-de-criacao/43dbhutmuh9m#> Acesso em: 23/06/2022.

PANDAY, U. S.; SHRESTHA, N.; MAHARJAN, S.; PRATIHAST, A. K.; SHANAWAZ; SHRESTHA, K. L.; ARYAL, J. Correlating the plant height of wheat with above-ground biomass and crop yield using drone imagery and crop surface model, a case study from Nepal. **Drones**, Basel, v. 4, n. 3, p. 1 – 15, 2020.

PÉLLICO NETTO, S.; BRENNA, D. A. **Inventário Florestal**. Curitiba, Paraná: UFPR, 1997, 316 p.

RIBEIRO, G. A.; SOARES, R. V. Caracterização do material combustível superficial e efeitos da queima controlada sobre sua redução em um povoamento de *Eucalyptus viminalis*. **Cerne**, Lavras, v. 4, n. 1, p. 58 - 72, 1998.

ROSSI, W. J. **Técnica de amostragem e análise de regressão**. Linbon, 1 ed. 2020, 326 p.

SANTOS, M. M.; BATISTA, A. C.; PEREIRA, A. D.; GANASSOLI NETO, E.; BARRADAS, A. C. S.; GIONGO, M. Characterization and dynamics of surface fuel of cerrado grassland in Jalapão region - Tocantins, Brazil. **Floresta**, Curitiba, v. 51, p. 127 - 136, 2021.

SANTOS, M. M.; MARTINS, T. S.; SILVA, D. B.; CACHOEIRA, J. N.; SANTOS, G. R.; GIONGO, M. Modelagem para estimativa de carga e umidade do material combustível em área de Cerrado. **Journal of Biotechnology and Biodiversity**, Gurupi, v. 7, n. 1, p. 249 - 256, 2019.

SEPLAN. Secretaria de Planejamento e Meio Ambiente do Estado do Tocantins. **Plano de Manejo do Parque Estadual do Cantão: Revisão**. Palmas: SEPLAN, 2016. Disponível em: <[http://gesto.to.gov.br/site\\_media/upload/plano\\_manejo/Plano\\_de\\_Manejo\\_-\\_PEC\\_-\\_2016.pdf](http://gesto.to.gov.br/site_media/upload/plano_manejo/Plano_de_Manejo_-_PEC_-_2016.pdf)>. Acesso em 28/08/2022

SEPLAN - Secretaria do Planejamento Superintendência do Planejamento e Gestão Central de Políticas Públicas. Diretoria de Zoneamento Ecológico-Econômico. **Base de dados geográficos do Tocantins**. 2012 Disponível em: <<https://www.to.gov.br/seplan/base-de-dados-geograficos-do-tocantins-atualizacao-2012/d7n1qsd70x2>> Acesso em: 27/07/2022.

SOARES, V. R.; BATISTA, C. A.; TETTO, A. F. **Incêndios Florestais: Controle, efeitos e uso do fogo**. Curitiba, Paraná: UFPR, 2 ed. 2017, 250 p.

SOUZA, I. V.; SANTOS, M. M.; GIONGO, M.; CARVALHO, E. V.; MACHADO, I. E. S. Estimativa do material combustível em área de Cerrado campo sujo a partir de imagens do sensor RGB. **Pesquisa Florestal Brasileira**, Colombo, v. 38, p. 1 - 6, 2018.

TAIZ, L.; ZEIGER, E. **Fisiologia e desenvolvimento vegetal**. Artmed Editora, Porto Alegre- RS. 6 ed. 2017, 888 p.

TAVARES, M. E. F. Metodologias usadas na quantificação de material combustível no Cerrado. **Vértices**, Campos dos Goytacazes, v. 19, n. 1, p. 175 - 182, 2017.

VOSELLMAN, G. Slope based filtering of laser altimetry data. **International Archives of Photogrammetry and Remote Sensing**, Hannover, v. 33, p. 935 - 942, 2000.

WHITE, B. L. A; RIBEIRO, G. T; SOUZA, R. M. O uso do BehavePlus como ferramenta para modelagem do comportamento e efeito do fogo. **Pesquisa Florestal Brasileira**, Colombo, v. 33, n. 73, p. 73 - 83, 2013.